

# On the Doping and Temperature Dependence of the Mass Enhancement Observed in the Cuprate $\text{Bi}_2\text{Sr}_2\text{CaCu}_2\text{O}_{8+\delta}$

P. D. Johnson<sup>1</sup>, T. Valla<sup>1</sup>, A. V. Fedorov<sup>1</sup>, Z. Yusof<sup>2</sup>, B. O. Wells<sup>2</sup>, Q. Li<sup>3</sup>, A. R. Moodenbaugh<sup>3</sup>, G. D. Gu<sup>4</sup>, N. Koshizuka<sup>5</sup>, C. Kendziora<sup>6</sup>, Sha Jian<sup>7</sup> and D. G. Hinks<sup>7</sup>

<sup>1</sup> *Department of Physics, Brookhaven National Laboratory, Upton, NY, 11973-5000*

<sup>2</sup> *Department of Physics, University of Connecticut, 2152 Hillside Road U-46, Storrs, CT 06269*

<sup>3</sup> *Division of Materials Sciences, Brookhaven National Laboratory, Upton, NY 11973*

<sup>4</sup> *School of Physics, University of New South Wales, P.O. Box 1, Kensington, New South Wales, Australia 2033*

<sup>5</sup> *Superconductivity Research laboratory, ISTEK, 10-13, Shinonome I- chrome, Koto-ku, Tokyo 135, Japan*

<sup>6</sup> *Materials Sciences Division, Naval Research Laboratory, Washington DC 20375*

<sup>7</sup> *Materials Sciences Division, Argonne National Laboratory, Argonne IL 60439*

High-resolution photoemission is used to study the electronic structure of the cuprate superconductor,  $\text{Bi}_2\text{Sr}_2\text{CaCu}_2\text{O}_{8+\delta}$ , as a function of hole doping and temperature. A kink observed in the band dispersion in the nodal or  $(0,0)$  to  $(\pi,\pi)$  direction in the superconducting state is associated with coupling to a resonant mode observed in neutron scattering. From the measured real part of the self energy it is possible to extract a coupling constant which is largest in the underdoped regime, then decreasing continuously into the overdoped regime.

(November 1, 2018)

In any system, electrons (or holes) may interact strongly with various excitations resulting in modifications to both their lifetime and binding energy. The quantity that describes these effects is the self-energy,  $\Sigma(\mathbf{k},\omega)$  the imaginary part representing the scattering rate or inverse lifetime, the real part, the shift in energy. An electron in a solid thus becomes "dressed" with a "cloud" of excitations, acquiring a different effective mass, but still behaving as a "single-particle" excitation or quasiparticle. This represents the traditional Fermi liquid (FL) picture. In more exotic materials, an electron or hole may lose its "single-particle" integrity and decay completely into collective excitations.

It has recently been demonstrated that angle-resolved photoemission (ARPES) is an excellent tool for momentum resolving self-energy effects. A measurement of the self-energy allows the determination of the coupling strength as well as the identification of the energy scale of the fluctuations involved in the coupling. As an example, self-energy effects due to the electron-phonon interaction have been identified in molybdenum [1] and beryllium [2]. In these cases the energy scale is represented by the Debye energy. More recently, in studies of the layered dichalcogenide  $2\text{H-TaSe}_2$ , self-energy corrections reflecting coupling to fluctuations in the charge density wave order parameter have been observed [3]. The extension of such studies to the realm of high- $T_c$  superconductivity allows the identification of the appropriate energy scales describing the fluctuations in these materials. It is not clear however, that a Fermi liquid methodology is appropriate for the high temperature superconductors (HTSC). Indeed in a recent study of optimally doped  $\text{Bi}_2\text{Sr}_2\text{CaCu}_2\text{O}_{8+\delta}$ , the non-Fermi liquid like nature of the material was demonstrated [4]. It was shown that

the imaginary part of the self-energy follows a Marginal Fermi liquid (MFL) behavior [5] with quantum critical scaling, suggesting the absence of any energy scale associated with the nodal excitations. However, in the same study [4], a change in the mass enhancement was observed in the superconducting state, indicating structure in the self-energy and the appearance of an energy scale well removed from the Fermi level. The corresponding change in the  $\text{Im}\Sigma$  was not observed directly. Subsequent experimental studies have reported that in the superconducting state the mass enhancement exists over a large portion of the Fermi surface [6,7]. Theoretical studies have focussed on the possibility that these observations reflect coupling to the magnetic resonance peak observed in neutron scattering studies [8].

In this paper, we examine the doping and temperature dependence of the mass enhancement. We find that in the normal state the self-energy is well described within the framework of the MFL model. However upon entering the superconducting state, changes occur in the ARPES spectra. We find that the self-energy correction and associated mass enhancement are strongly dependent on the hole doping level, decreasing continuously with doping. Further the energy scale observed in the superconducting state is linearly dependent on the transition temperature  $T_C$ . This dependence is almost identical to that observed for the resonant collective mode observed in neutron scattering studies [9,10].

The experimental studies reported in this paper were carried out on a photoemission facility equipped with a Scienta electron spectrometer [11]. In this instrument, the total spectral response may be measured as a function of angle and energy simultaneously with a momentum resolution of  $\sim 0.005 \text{ \AA}^{-1}$  and an energy resolution

of  $\sim 10$  meV. Photons were provided by a Normal Incidence Monochromator based at the National Synchrotron Light Source. Samples of optimally doped ( $T_C = 91$  K)  $\text{Bi}_2\text{Sr}_2\text{CaCu}_2\text{O}_{8+\delta}$  were produced by the floating zone method [12]. The underdoping and overdoping was achieved by annealing optimally doped samples in argon [13] and in oxygen [14], respectively. All samples were mounted on a liquid He cryostat and cleaved *in-situ* in the UHV chamber with base pressure  $3 \times 10^{-9}$  Pa. The sample temperature was measured using a calibrated silicon sensor. The self-energy corrections were determined either from energy distribution curves (EDC) or from momentum distribution curves (MDC). The EDC represents a measure of the intensity as a function of binding energy at constant momentum and the MDC a measure of the intensity as a function of momentum at constant binding energy.

In Fig. 1 we show the photoemission intensities recorded as a function of binding energy and momentum in the (0,0) to  $(\pi, \pi)$  direction of the Brillouin zone for from left to right, the underdoped (UD), optimally doped (OP) and overdoped (OD)  $\text{Bi}_2\text{Sr}_2\text{CaCu}_2\text{O}_{8+\delta}$  samples, all in the superconducting state. In the lower panel we show the corresponding band dispersions obtained from MDC's for the superconducting and normal states. It is clear that even in the normal state, the dispersion in the vicinity of the Fermi level deviates from the linear dispersion predicted by first-principles band structure calculations [15]. In the superconducting state, an additional modification to the dispersion develops for the under- and optimally doped samples. In the overdoped material there is no detectable change in dispersion.

The spectra in Fig. 1 display other interesting features. For  $\omega \geq 50$  meV the velocity, or rate of band dispersion decreases with doping. This is surprising because one might anticipate the velocity decreasing as the states became more localized in the underdoped regime. Secondly, the spectral response is less well defined in the underdoped regime with the spectral width in both energy and momentum exceeding the amount of dispersion from  $k = k_F$ . Following recent suggestions of Orgad *et al.* [16] these two observations may be evidence of increased electron (hole) fractionalization in the underdoped regime.

In Fig. 2 we show the deviation,  $\text{Re}\Sigma$ , from the non-interacting dispersion as a function of binding energy for the three doping levels for both the superconducting and normal states. We define the non-interacting dispersion as a straight line that coincides with the experimentally measured Fermi wave- vector and the dispersion measured at a higher binding energy, typically 250 meV, as indicated in Fig. 1. The real part of the self-energy is set to zero at these points. The overall magnitude of the self-energy continuously decreases with doping in both the normal and superconducting state. We also show the difference in  $\text{Re}\Sigma$  between the superconducting state and normal state. We suggest that this difference repre-

sents a change in the excitation spectrum associated with the coupling upon entering the superconducting state. This change should also be manifested in measurements of  $\text{Im}\Sigma$ . While apparent in the underdoped regime [17], the effect is too subtle to observe directly in the optimally doped material.

In Fig. 3 we plot different quantities deduced from  $\text{Re}\Sigma$  as a function of the deviation from the maximum  $T_C = 91$  K, characterizing the optimally doped material. In panel (a) we plot both  $\omega_0$ , the energy of the maximum in  $\text{Re}\Sigma$  in the superconducting state and  $\omega_0^{sc}$ , the energy of the maximum in the difference between the superconducting- and normal-state. Since in the overdoped regime the difference between the superconducting- and normal- state dispersion vanishes, the energy scale characterizing the superconducting state could not be detected in the nodal region. The characteristic energy was therefore identified only for a limited range of overdoping and only by moving away from the node towards the  $(\pi, 0)$  region where the coupling is observed to be stronger while the characteristic energy of the kink remains momentum-independent [7,18]. Indeed, measurements of the renormalized velocity in the superconducting state indicate that, for optimal doping, the coupling increases by a factor of 3 or more on moving towards the  $(\pi, 0)$  region [18]. In the overdoped regime, there is also more uncertainty in the transition temperature due to the increased tendency of losing oxygen [19].

In the underdoped regime it is clear that the characteristic energies  $\omega_0$  and  $\omega_0^{sc}$  scale linearly with  $T_C$  as opposed to, for instance the magnitude of the maximal gap observed in these materials. The latter increases continuously on going into the underdoped regime [20]. When fitted with a straight line, the data points for  $\omega_0^{sc}$  and  $\omega_0$  in Fig. 3(a) yield  $\omega \sim 6k_B T_C$ . This behavior is reminiscent of that reported in neutron scattering studies where all the characteristic low-energy features in the superconducting state appear to scale with  $T_C$ . In particular, the resonance energy,  $E_r$ , was found to scale as  $E_r \sim 5.4k_B T_C$  [10], while the spin gap scales as  $\Delta_s \sim 3.8k_B T_C$  [21]. The possibility that the kink reflects coupling to zone boundary longitudinal optical phonons has also been discussed in the literature [22]. However, recent neutron studies indicate that these phonons occur at the same energy, independent of doping [23]. This is in complete contrast to the doping dependence of the kink energy observed in the present study.

The real part of the self energy may also be used to extract the coupling strength to the excitations involved in the coupling [24] via  $\lambda = -(\partial \text{Re}\Sigma / \partial \omega)_{E_F}$ , neglecting momentum dependence of the self energy in the narrow interval around  $k_F$ . The coupling constant  $\lambda$  is simply obtained by fitting the low energy part of  $\text{Re}\Sigma(\omega)$  to a straight line. In Fig. 3(b) we plot  $\lambda$  for different samples in the superconducting state as a function of  $T_C$ . From the figure we see that the coupling decreases continuously

with increasing doping level, reflecting the latter rather than the transition temperature.

Shown in Fig. 4, the "kink" and the magnetic resonance mode also display the same temperature dependence. Here the temperature dependence of  $\text{Re}\Sigma$  for the underdoped (UD69K) sample, measured at the characteristic energy  $\omega = \omega_0^{\text{sc}}$ , is compared with the intensity of the resonance mode measured in inelastic neutron scattering (INS) from an  $\text{YBa}_2\text{Cu}_3\text{O}_{6+x}$  sample with similar  $T_C$  [9]. Although our comparison is between two different systems, we note that a recent INS study combined with ARPES on the same underdoped  $\text{Bi}_2\text{Sr}_2\text{CaCu}_2\text{O}_{8+\delta}$  sample ( $T_C = 70$  K) have reported results nearly identical to the present study [25]. The identical temperature dependence in Fig. 4 points to a common origin for both phenomena. Note that both features exist at temperatures significantly higher than  $T_C$ . The temperature range over which they lose intensity at the fastest rate appears close to  $T_C$ . However the features show intensity up to temperatures close to  $T^*$ , the pseudo-gap temperature measured in various transport properties.

We have provided strong evidence that in the superconducting state the low-energy excitations are affected by the low-energy part of spin fluctuation spectrum observed in neutron scattering. The question naturally arises as to what is responsible for the mass enhancement observed in the normal state for all samples. If phonons were the source of coupling, we might anticipate a *saturation in the scattering rate at frequencies greater than the Debye frequency and a marked temperature dependence in that range* [1,2,24]. This is clearly in contrast with optical conductivity [26] and photoemission [4,6,7] experiments on the optimally- and underdoped samples, where the obvious lack of saturation in the scattering rate points to the absence of a well-defined cutoff in the excitation spectrum. Phonons, on the other hand, are *always* limited to a finite energy range (usually  $\leq 100$  meV in these materials). Further, as we have noted earlier, no significant temperature and doping dependence is observed in the phonon spectrum. More likely is the possibility that the enhancement still reflects coupling to spin excitations and that the spectrum of excitations changes with temperature. Indeed, the spin response changes between the normal and (pseudo)gapped state. A spin gap opens at low energies in superconducting state, and the strong resonance mode appears at commensurate momenta,  $\mathbf{Q} = (\pi, \pi)$ . The spectrum becomes incommensurate for lower and higher energies. These temperature changes in the susceptibility are in one-by-one correlation with the temperature changes in the single-particle spectrum. The stronger the temperature change in susceptibility, the stronger the temperature change in photoemission. This suggests that in the overdoped regime, not only the susceptibility weakens, but also that the change between the normal- and superconducting- states gradually disappears. In systems

where the "resonance mode" dominates the susceptibility in the superconducting state, coupling to it causes the "kink" in the dispersion at roughly the same energy [27]. If in the normal state the coupling still reflects spin fluctuations, it should scale with the spin susceptibility  $\chi''$ . Indeed, the spin susceptibility has been shown to increase in the underdoped region in both the normal and superconducting states [28], consistent with the present findings. As a two-particle response function, it is only limited by the band width, in accord with the absence of a clear cutoff in the single-particle scattering rate.

The Kramers Kronig transform of a scattering rate,  $\text{Im}\Sigma \propto \omega$  gives  $\text{Re}\Sigma = g'\omega \ln(\omega_c/\omega)$ , where  $g'$  is a coupling constant and  $\omega_c$  is a high-energy cutoff as defined within the MFL framework [5]. Indeed, any system with the scattering rate linear in binding energy should also display a logarithmic correction to the dispersion. Fitting the  $\text{Re}\Sigma$  shown in the Fig. 2 gives a value of approximately 230 meV for  $\omega_c$  and values for  $g'$  of 0.54, 0.29 and 0.24 for the underdoped, optimally doped and overdoped samples respectively. We note that the value obtained for  $g'$  for the optimally doped material is consistent with the  $\omega$  dependence of  $\text{Im}\Sigma$  found in our earlier study [4] and is in good agreement with values obtained in a recent analysis of normal state EDCs by Abrahams and Varma [29]. The observation that the MFL form for the self energy fits the data in the overdoped region in both the normal and superconducting state is suggestive that the quantum critical point, if it exists, may well be displaced towards the overdoped region.

To conclude, the doping, temperature and momentum dependences of the various characteristic features seen in the cuprate photoemission spectra are consistent with a picture where the injected hole couples to the spin fluctuations observed in INS. Indeed this evidence showing that the mass enhancement associated with the opening of the (pseudo)gap is electronic in nature is reminiscent of the behavior reported for 2H-TaSe<sub>2</sub> [3]. In the latter study a mass- enhancement or kink in the dispersion developed with the formation of the CDW gap. The energy scale, being much larger than the Debye energy, was attributed to electronic excitations across the CDW gap. In the present study, from the observation that in the underdoped region the transition temperature  $T_C$  decreases as the coupling increases, we conclude that the coupling strength alone is clearly insufficient to explain the superconductivity in these materials and that some other ingredients, such as the carrier concentration [17,30] and the phase coherence [31,32], are clearly required.

The authors would like to acknowledge useful discussions with Alexei Tsvelik, Andy Millis, V.N. Muthukumar, Dimitri Basov, Andrey Chubukov, John Tranquada, Steve Kivelson and Takeshi Egami. The work was supported in part by the Department of Energy under contract number DE-AC02-98CH10886 and in part by the New Energy and Industrial Technology Development Or-

- 
- [1] T. Valla, A. V. Fedorov, P. D. Johnson and S. L. Hulbert, *Phys. Rev. Lett.* **83**, 2085 (1999).
- [2] M. Hengsberger *et al*, *Phys. Rev. Lett.* **83**, 592 (1999); S. LaShell, E. Jensen and T. Balasubramanian, *Phys. Rev. B* **61**, 2371 (2000).
- [3] T. Valla *et al*, *Phys. Rev. Lett.* **85**, 4759 (2000).
- [4] T. Valla *et al*, *Science* **285**, 2110 (1999).
- [5] C. M. Varma *et al*, *Phys. Rev. Lett.* **63**, 1936 (1989).
- [6] P. V. Bogdanov *et al*, *Phys. Rev. Lett.* **85**, 2581 (2000).
- [7] A. Kaminski *et al*, *Phys. Rev. Lett.* **86**, 1070 (2001).
- [8] M. Eschrig and M. R. Norman, *Phys. Rev. Lett.* **85**, 3261 (2000).
- [9] P. Dai *et al*, *Science* **284**, 1346 (1999).
- [10] H. F. Fong *et al*, *Nature* **398**, 588 (1999); H. He *et al*, *Phys. Rev. Lett.* **86**, 1610 (2001).
- [11] P. D. Johnson *et al*, *Proceedings of the 11<sup>th</sup> Synch. Rad. Conf.* AIP Press NY, **521**, 73 (2000).
- [12] G. D. Gu, K. Takamaku, N. Koshizuka and S. Tanaka, *J. Crystallogr. Growth* **130**, 325 (1990); N. Miyakama *et al*, *Phys. Rev. Lett.* **80**, 157 (1998).
- [13] A. R. Moodenbaugh, D. A. Fisher, Y. L. Wang and Y. Fukumoto, *Physica C* **268**, 107 (1996).
- [14] C. Kendziora, R. J. Kelley, E. Skelton, and M. Onellion, *Physica C* **257**, 74 (1996).
- [15] H. Krakauer and W. E. Pickett, *Phys. Rev. Lett.* **60**, 1665 (1988).
- [16] D. Orgad *et al*, cond-mat/0005457.
- [17] T. Valla *et al*, to be published.
- [18] T. Valla *et al*, *Phys. Rev. Lett.* **85**, 828 (2000).
- [19] To minimize uncertainties for the overdoped samples,  $T_C$  was measured in situ, by monitoring the superconducting gap and by measuring the susceptibility before and after the photoemission.
- [20] J. C. Campuzano *et al*, *Phys. Rev. Lett.* **83**, 3709 (1999).
- [21] P. Dai, H. A. Mook, R. D. Hunt and F. Doğan, *Phys. Rev. B* **63**, 054525 (2001).
- [22] A. Lanzara *et al*, cond-mat/0102227; Z.-X. Shen, A. Lanzara and N. Nagaosa, cond-mat/0102244.
- [23] Y. Petrov *et al*, cond-mat/0003414; R. J. McQueeney *et al*, cond-mat/0105593.
- [24] G. D. Mahan, *Many Particle Physics* (Plenum Press, New York 1991).
- [25] J. Mesot *et al*, cond-mat/0102339.
- [26] A. V. Puchkov, D. N. Basov, and T. Timusk, *J. Phys. Condens. Matter* **8**, 10049 (1996).
- [27] Coupling to an Einstein-like mode results in a peak in the real part of the self energy at that energy.
- [28] P. Bourges, in *The Gap symmetry and Fluctuations in High Temperature Superconductors*, ed. By J. Bok, G. Deutscher, D. Pavuna, and S.A. Wolf (Plenum Press, 1998).
- [29] E. Abrahams and C. Varma, *Proc. Natl. Acad. of Sciences* **97**, 5714 (2000).

- [30] H. Ding *et al*, cond-mat/0006143.
- [31] V. J. Emery and S. A. Kivelson, *Nature* **374**, 434 (1995).
- [32] I. Vobornik *et al*, *Phys. Rev. Lett.* **82**, 3128 (1999); *Phys. Rev. B* **61**, 11248 (2000).

FIG. 1. Upper panels:- Two dimensional photoemission intensities observed from (a) underdoped (UD), (b) optimally doped (OP) and (c) overdoped (OD)  $\text{Bi}_2\text{Sr}_2\text{CaCu}_2\text{O}_{8+\delta}$  samples. The superconducting transition temperatures are indicated. Lower panels:- The dotted lines indicate the MDC deduced dispersions for both the superconducting (blue dots) and normal states (open red diamonds) corresponding to the different samples in the panels above.

FIG. 2.  $\text{Re}\Sigma$  as a function of binding energy for the superconducting (blue dots) and normal states (open red diamonds) for the underdoped (UD), optimally doped (OP) and overdoped (OD) samples, as indicated. The solid lines through the normal state data represent MFL fits to the data. The difference between the superconducting and normal  $\text{Re}\Sigma$  for each level of doping is also plotted (green triangles). The lines through the latter are Gaussian fits to extract the peak energy  $\omega_0^{sc}$ .

FIG. 3. (a) Plot of  $\omega_0$ , the energy of the maximum value of  $\text{Re}\Sigma$  in the superconducting state (open squares), and  $\omega_0^{sc}$  (solid circles), the energy of the maximum in difference between the superconducting and normal state values plotted as a function of  $T_C$  referenced to the maximum  $T_C^{max}$  ( $\sim 91$  K). (b) The coupling constant  $\lambda$ , determined as described in the text and plotted as a function of  $T_C$ .

FIG. 4. Temperature dependence of  $\text{Re}\Sigma(\omega_0^{sc})$  from the nodal line for the UD69K sample (black squares) compared with the temperature dependence of the intensity of the commensurate resonance mode observed in neutron scattering studies of underdoped  $\text{YBa}_2\text{Cu}_3\text{O}_{6+x}$ ,  $T_C = 74$  K, (ref. [9]) (gray circles).

Fig. 1

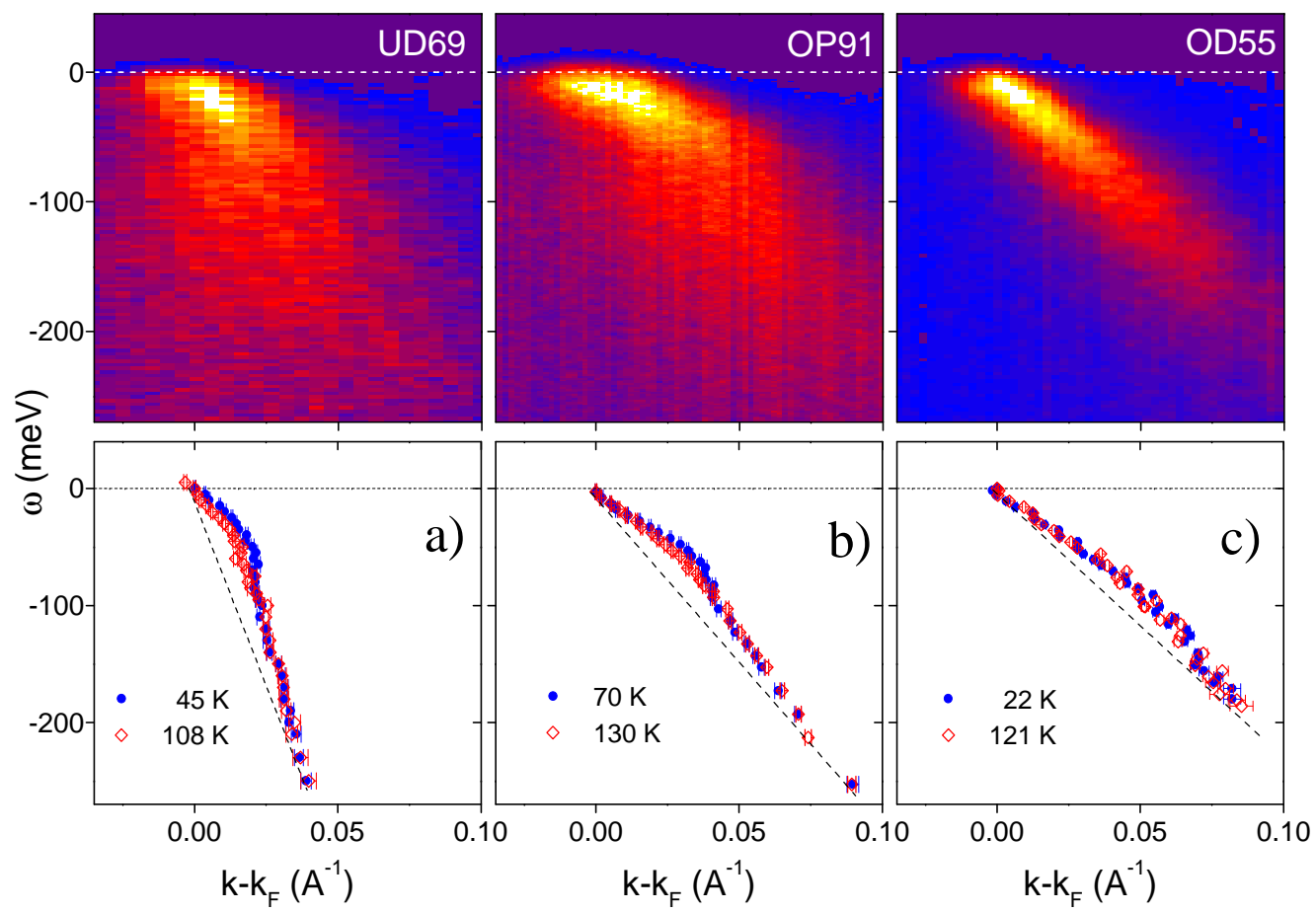


Fig. 2

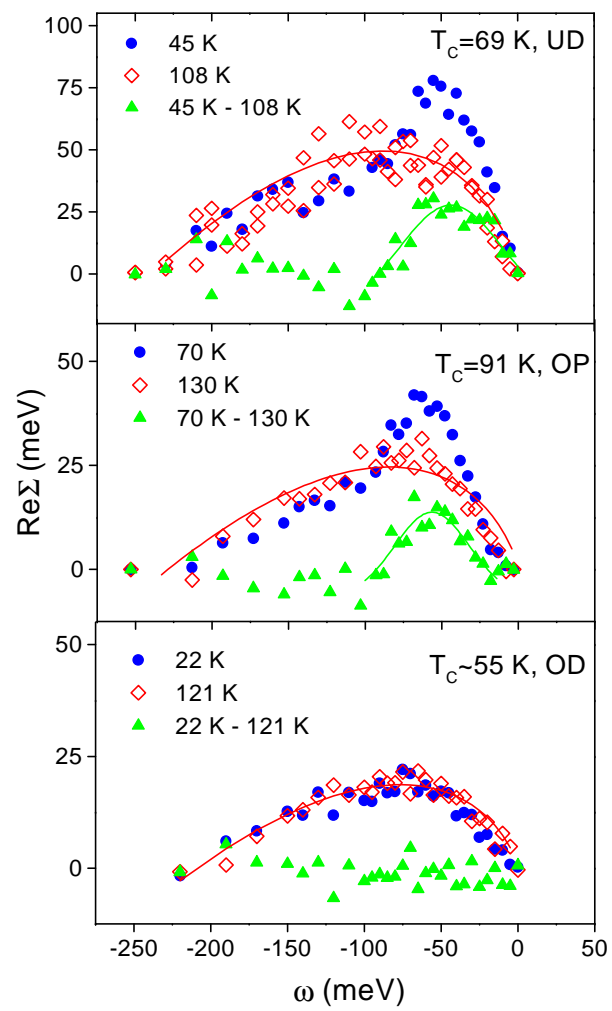


Fig. 3

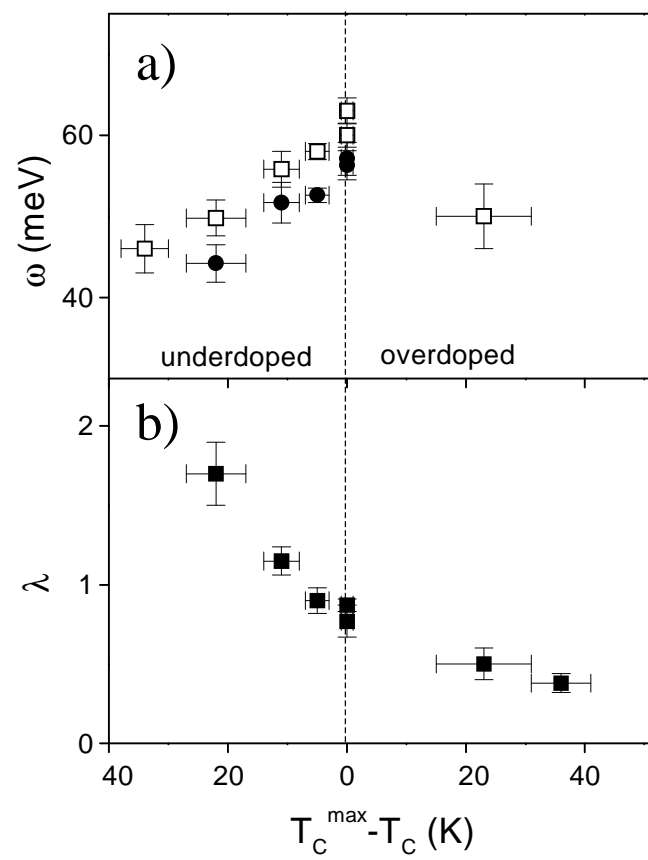


Fig. 4

